.

The correlation between electric field emission phenomenon and Schottky contact reverse bias characteristics in nanostructured systems

J. Yu , J. Liu, M. Breedon, M. Shafiei, H. Wen, Y. X. Li, W. Wlodarski, G. Zhang, and K. Kalantar-zadeh

Citation: Journal of Applied Physics **109**, 114316 (2011); doi: 10.1063/1.3583658
View online: http://dx.doi.org/10.1063/1.3583658
View Table of Contents: http://aip.scitation.org/toc/jap/109/11
Published by the American Institute of Physics

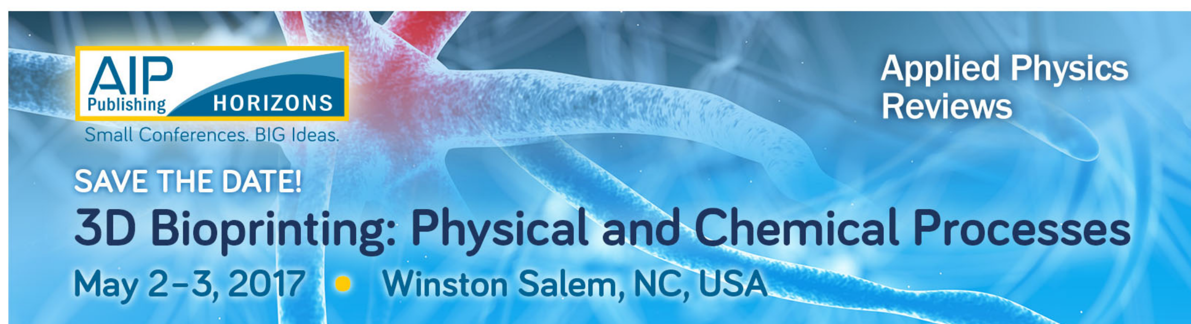

The correlation between electric field emission phenomenon and Schottky contact reverse bias characteristics in nanostructured systems

J. Yu,[1,a)] J. Liu,[2] M. Breedon,[1] M. Shafiei,[1] H. Wen,[3] Y. X. Li,[3] W. Wlodarski,[1] G. Zhang,[2] and K. Kalantar-zadeh[1]

[1]*Department of Electrical and Computer Engineering, RMIT University, GPO Box 2476, Melbourne 3001, Australia*

[2]*Key Laboratory for the Physics and Chemistry of Nanodevices, Department of Electronics, Peking University, Beijing 100871, People's Republic of China*

[3]*Shanghai Institute of Ceramics, Chinese Academy of Sciences, Shanghai 200050, People's Republic of China*

(Received 27 December 2010; accepted 29 March 2011; published online 13 June 2011)

Two different morphologies of nanotextured molybdenum oxide were deposited by thermal evaporation. By measuring their field emission (FE) properties, an enhancement factor was extracted. Subsequently, these films were coated with a thin layer of Pt to form Schottky contacts. The current-voltage (*I-V*) characteristics showed low magnitude reverse breakdown voltages, which we attributed to the localized electric field enhancement. An enhancement factor was obtained from the *I-V* curves. We will show that the enhancement factor extracted from the *I-V* curves is in good agreement with the enhancement factor extracted from the FE measurements.
© *2011 American Institute of Physics*. [doi:10.1063/1.3583658]

I. INTRODUCTION

Research and development in nanofabrication has produced many new devices taking advantage of nanodimensional tips and edges with enhanced electric and optical properties.[1,2] In particular, nanostructured metals or metal oxides with sharp morphologies can adapt the ambient electric field to produce locally enhanced electric fields in proximity to the sharp tips and edges.[3,4] Such a large localized field enhancement plays an important role in developing devices with extraordinary capabilities. Two of these nanostructured devices are "field emitters" and "Schottky contacts in reverse bias." Such a field enhancement in nanoscale devices has also been suggested to be a vital component in surface enhanced Raman scattering.[5,6]

Metals or metal oxides that can be engineered into nanodimensional tips and edges to function as field emitters, can achieve a higher rate of electron tunneling, and produce high local current densities.[7] It is known that the low densities of states at the sharp edges also cause the emitted electrons to be highly coherent and mono-energetic,[8] which can be used as efficient low energy electron point sources for microscopy applications.[6] In addition, the phenomenon can also be incorporated in panel display devices and high brightness electron sources.[9] The enhanced emission phenomenon is defined by its "field enhancement factor," γ_a, which relates the ambient and localized electric fields.

In nanostructured Schottky contacts, the current-voltage (*I-V*) characteristics considerably differ from the characteristics exhibited by conventional thin film Schottky contacts.[10] Such a difference is more pronounced in the reverse bias condition than in forward bias, as the contacts have high breakdown voltages in reverse bias that is not seen in conventional devices.[11] We previously showed the extraordinary capability of such devices in reverse bias for applications such as gas sensing. We also extracted equations that explains the operation of these devices using a "field enhancement factor," $\gamma_{Schottky\text{-}a}$, which attributes to the enhancement of electric field at the surface of nanostructures such as MoO_3 and ZnO.[4,12]

In this paper, we will show the two "field enhancement factors," which are obtained from the field emission measurements and Schottky contact *I-V* characteristics in reverse bias, are closely related. Extracting the value for the "enhancement factor" from Schottky contact *I-V* curves, rather than field emission measurements, can be advantageous and facile. The field emission measurements are generally dependent upon the distance at which the emission is measured. They require applying high magnitudes of voltage (in the order of kilovolts) and must also be performed under very low atmospheric pressures, which require expensive equipment. Such harsh measurement environments can deteriorate the morphology of the specimen during the experimentation and result in inaccuracies. Instead, Schottky contact measurements can be performed in direct contact with the specimen surface and is free of rigorous conditions.

We measure the field emission generated by MoO_3 nanostructured films and calculate the corresponding enhancement factor γ_a. For the purpose of this investigation, MoO_3 was chosen as it is a versatile material and can be synthesized in many different morphologies.[13,14] MoO_3 nanostructures can be easily fabricated with sharp structures, ideally suited to generate strong localized electric fields.[12] Subsequently, we develop Pt/nanostructured MoO_3 Schottky contacts to calculate a different enhancement factor $\gamma_{Schottky\text{-}a}$ by curve fitting the Schottky contact *I-V* equations to the reverse *I-V* characteristics. From these measurements, we will show that the enhancement factor γ_a, which is extracted in the field emission measurements, is in good agreement with $\gamma_{Schottky\text{-}a}$ that is extracted from the *I-V* curves in nanostructured Schottky contacts.

[a)]Electronic mail: j.yu@student.rmit.edu.au

0021-8979/2011/109(11)/114316/4/$30.00 © 2011 American Institute of Physics

II. EXPERIMENTAL

Nanotextured MoO_3 with two distinctly different morphologies were deposited on SiC substrates using thermal evaporation (see "supplementary information" for the deposition conditions and characterization of materials[15]). The analysis of the morphology of the '770 °C' MoO_3 nanostructures revealed randomly orientated nanostructures such as nanoplatelets with thicknesses up to 500 nm, lengths and widths from 2 to 3 μm and nanoplatelets that are stacked in a towering formation with side lengths ranging between 150 nm to 1 μm and their heights ranging from 1 μm to several μm [Fig. 1(a)]. Also the presence of nanowires was observed with diameters between 25 to 100 nm, and lengths ranging between 500 nm to 3 μm.

The '850 °C' nanostructures consisted of larger, sharper, and more well defined structures such as nanoplatelets with dimensions ranging between 1 to 10 μm with no presence of nanowires [Fig. 1(b)]. As the result of elevating the deposition temperature to 850 °C, the growth of the larger structures was observed that can be attributed to Ostwald ripening behavior.[16]

The most important parameters that reflect the emission capability of a cold electron source are the turn-on field (E_{to}) and the threshold field (E_{th}). They are defined as the fields that extract 10 μA/cm^2 and 1 mA/cm^2, respectively. We measured the E_{th} of 1 mA/cm^2 as it is usually considered sufficient for practical applications in field emission displays.[17] The current density *J-E* characteristics of both the samples '770 °C' and '850 °C' are shown in Fig. 2. The plot of ln(J/E^2) versus $1/E$ is shown in the inset of Fig. 2. Field emission measurements were conducted at room temperature.

From these plots we determined the field emission turn-on field (E_{to}) for samples '770 °C' and '850 °C' as 12.4 and 11.1 V/μm, respectively. The lower turn-on field exhibited by the nanostructures in '850 °C' has been attributed to the sharp and well-defined nanostructures, favorable for producing low threshold field emission. Nanostructures in '770 °C' had a comparatively rounder and smoother morphologies, which explains the larger E_{to} required to induce the same magnitude of field emission.

Wei *et al.*[18] reported a turn-on field of ~4.3 V/μm for thin MoO_3 nanoflowers. Similarly, a turn-on field of 13.2 V/μm was reported by Li *et al.*[3] with MoO_3 nanobelts at 50 μm spacing and 8.7 V/μm at a spacing of 80 μm between the anode and the cathode. However, in general, it is difficult to perform a direct comparison of the turn-on fields as the field emission properties in literature can vary significantly due to the fact that measurements were taken at different electrode interspacings.

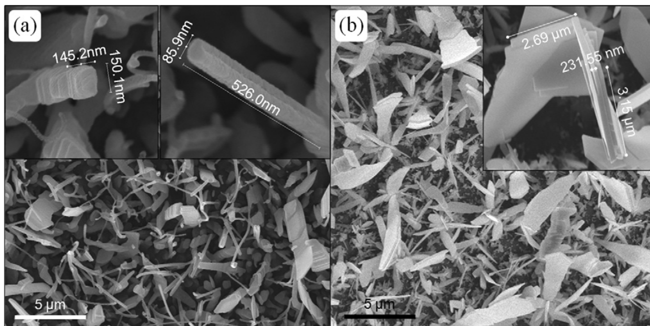

FIG. 1. SEM of the MoO_3 nanostructures deposited by thermal evaporation at (a) 770 °C and (b) 850 °C.

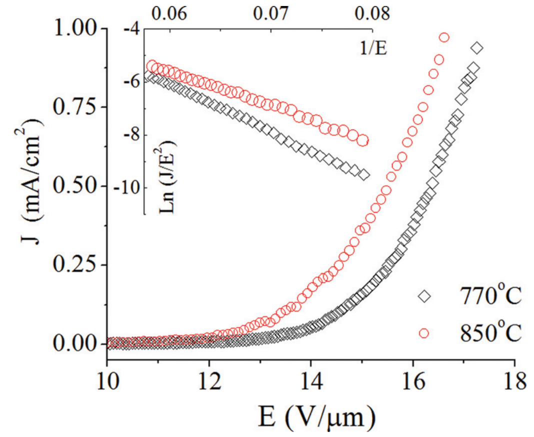

FIG. 2. (Color online) Plot of J-E field emission characteristics (inset showing the Ln (J/E^2) curves) from the MoO_3 nanostructures.

According to field emission theory, the *J-E* characteristic equation is given by[19]

$$J = \frac{1.56 \times \gamma_a^2 E^2}{\Phi} \exp\left(-\frac{6.83 \times 10^3 \Phi^{3/2}}{\gamma_a E}\right), \tag{1}$$

where J is the current density (A/cm^2), Φ is the work function of MoO_3 assumed as 5.68 eV,[20] γ_a is the field enhancement factor, and E is the average local electric field (V . m^{-1}) at the emission sites.

As can be seen in Fig. 2(b), a straight line was obtained in the ln(J/E^2) curve which implies that the field emission from these nanostructures follow the Fowler-Nordheim (FN) equation:[19]

$$\ln\left(\frac{J}{E^2}\right) = -\frac{6.83 \times 10^3 \Phi^{3/2}}{\gamma_a} \times \frac{1}{E}. \tag{2}$$

As defined using the FN theory, the slope of the ln(J/E^2) versus $1/E$ plot determines the enhancement factor γ_a and the intercept varies with the effective emission area. By substituting the assumed work function into Eq. (2), the enhancement factors were calculated as 590 and 750 for the '770 °C' and '850 °C' samples, respectively. We associate these numerical results to the difference in the surface morphology. The results indicated that the '850 °C' nanostructures produced a higher field enhancement factor as sharp, well-defined nanoplatelet structures were present. For comparison, a summary of the available literature for field emission enhancement based on nanotextured MoO_3 materials is presented in Table I-S in the supplementary materials.[15]

In order to calculate the enhancement factor using the Schottky contact method, the *I-V* characteristics of Pt/MoO_3 nanostructured Schottky contacts were measured (Fig. 3). The inset in Fig. 3 shows breakdown voltages of −5.77 and −5.17 V, at a current of −10 μA, for the '770 °C' and

TABLE I. Comparison of the field enhancement factors.

Field enhancement factor	770 °C	850 °C
Measured via field emission	590	750
Curve fitted to the measured *I-V* characteristics	720	880

'850 °C' Schottky contacts, respectively. To correlate with field emission measurements, the *I-V* characteristics were also obtained at room temperature.

In the region of less than the breakdown threshold (current less than $-10\ \mu$A), the *I-V* curves of the '700 °C' contacts exhibit a higher voltage than that of the '850 °C' contacts. Above the breakdown threshold the two curves reaches a crossover point (at a current of $-20\ \mu$A) at ~6.6 V. In the region subsequent to the crossover point, the *I-V* curves of the '850 °C' contacts exhibit a higher voltage than that of the '700 °C' contacts.

In a Schottky contact, the forward bias current density is given by[21]

$$J_F = A^{**}T^2 \exp\left[-\frac{q\phi_{B0}}{kT}\right] \exp\left[\frac{q(\Delta\phi + V)}{kT}\right], \qquad (3)$$

where, J_F is the magnitude of the forward current density, A^{**} is the effective Richardson constant, T is the absolute temperature, q is the charge constant, ϕ_{B0} is the barrier height, and k is the Boltzmann constant. The reverse bias current density is given by[21]

$$J_R \approx A^{**}T^2 \exp\left[-\frac{q\left(\phi_{B0} - \sqrt{q\xi_m/4\pi\varepsilon_s}\right)}{kT}\right], \qquad (4)$$

where J_R is the magnitude of the reverse current density, ξ_m is the maximum localized electric field, and ε_s is the permittivity of the metal oxide.

For nanostructured materials, the maximum localized electric field ξ_m is a function of V_R as[22]

$$\xi_m = \gamma_{\text{Schottky-a}} \sqrt{\frac{2qN_D}{\varepsilon_s}\left(|V_R| + \psi_{bi} - \frac{kT}{q}\right)}, \qquad (5)$$

where $\gamma_{\text{Schottky-a}}$ is the enhancement factor, N_D is the number of carriers, which is assumed as 10^{20} cm^{-3} for nanotextured MoO_3,[22] V_R is the reverse bias voltage, and ψ_{bi} is the built in voltage.

Sharp nanostructures can adapt ambient electric fields to produce localized electric fields and we determined the enhancement factors by curve fitting Eqs. (4) and (5) to the *I-V* data measured from the '770 °C' and '850 °C' contacts, as shown in Fig. 4. The curve fitting is performed by plotting Eqs. (4) and (5) on the same graph as the measured *I-V* data. The parameters: (a) effective Richardson constant, (b) the number of carriers, and most importantly (c) the enhancement factor were varied individually until the closest fit of the Eq. (4) could be observed with the measured *I-V* data.

The curve fitting calculated the enhancement factors for the respective samples '770 °C' and '850 °C' Schottky contacts as 720 and 880, respectively. The curve fitting to the '770 °C' Schottky contact *I-V* data is shown in Fig. 4 and although there are slight differences in the fit at relatively low and significantly high voltages, it is still quite a good fit. The curve fitting also correlates well with the *I-V* data measured from '850 °C' Schottky contact *I-V* curves as seen in Fig. 4.

The enhancement factors extracted from the field emission and Schottky contacts are shown in Table I. It can be seen that enhancement factors calculated from the Schottky contact measurements are slightly larger than the field emission experiments extracted values, which can be attributed to the overestimation in the curve fitting. Previously the authors obtained $\gamma_{\text{Schottky-a}}$ value of ~1000 by curve fitting to the *I-V* characteristics for MoO_3 nanoplatelets with very sharp edges.[22] This can be expected, as the curve fitted enhancement factor from the MoO_3 structures is larger for the '850 °C' sample than the factor for the '770 °C' sample due to the presence of the sharp corners in the nanostructures morphology.

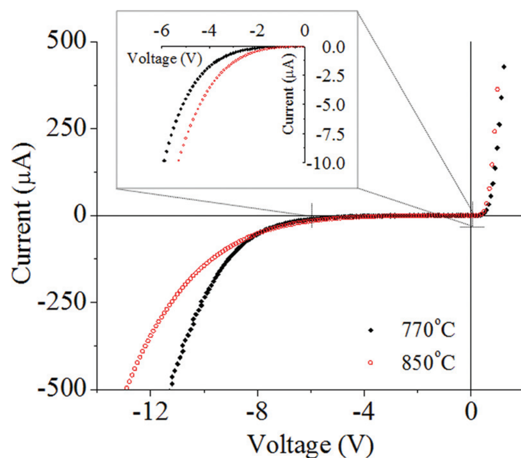

FIG. 3. (Color online) *I-V* characteristics of Pt/MoO_3 nanostructured Schottky contacts at 25 °C.

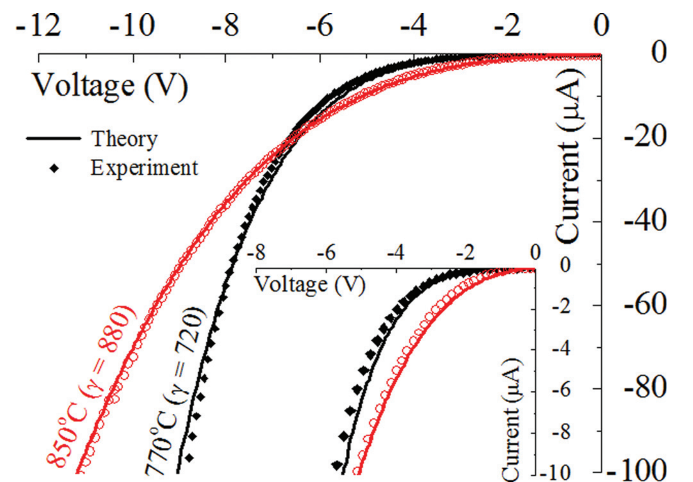

FIG. 4. (Color online) Comparison of theoretical and experimental *I-V* characteristics of '770 °C' and '850 °C'. Inset shows the *I-V* curves on a scale from 0 to $-10\ \mu$A.

As extra information for the readers, the Schottky barrier heights in the forward and reverse bias conditions of the nanostructured Pt/MoO_3 contacts are also calculated and presented in the supplementary.[15]

From the measured *I-V* characteristics, the magnitude of the forward Schottky barrier height was calculated as 645 and 640 meV for the 770 and 850 °C nanostructured diodes, respectively. These are rather large magnitudes, for which the thermionic emission mechanism is dominant.[4,23] The magnitude of the reverse bias barrier height was calculated as 698 and 650 meV for the same two nanostructured diodes. As described previously, when an external field is applied across the Pt/MoO_3 nanostructured diodes, the MoO_3 adapts the ambient field to produce localized electric fields. As these extremely strong localized electric field forces are present, they push the electrons over the barrier. This may be described as a virtual lowering of the reverse Schottky barrier height. However, the actual barrier height does not change to induce thermionic emission. Therefore, the tunneling contribution to the electron transport still exists and the electric field also contributes to it further by strengthening it due to this strong electric force.

III. CONCLUSION

In conclusion, we devised a method of extracting the enhancement factor for field emission of a nanostructured film by using reversed bias *I-V* characteristics of nanostructured Schottky contacts, which was built on the same film. The enhancement factor measured from the nanostructured MoO_3 Schottky contacts formed at 770 °C and 850 °C were calculated as 720 and 880, respectively. The corresponding values from the field emission measurements were 590 and 750, respectively, which show that the enhancement factors obtained using the two different methods were in good agreements. Although the *I-V* curve fitting technique is an approximation, it is proved to be a quick and simple method in determining the enhancement factor, which can be applied in assessing the performance of field emission devices.

ACKNOWLEDGMENTS

This work was supported partly by the Ministry of Science and Technology of the People's Republic of China (Contract No. 2007CB936204) and the National Natural Science Foundation of China (No. 61076057).

[1] Y. Wu, J. Xiang, C. Yang, W. Lu, and C. M. Lieber, Nature **430**, 61 (2004).
[2] J. Michaelis, C. Hettich, J. Mlynek, and V. Sandoghdar, Nature **405**, 325 (2000).
[3] Y. B. Li, Y. Bando, D. Golberg, and K. Kurashima, Appl. Phys. Lett. **81**, 5048 (2002).
[4] J. Yu, S. J. Ippolito, W. Wlodarski, M. Strano, and K. Kalantar-Zadeh, Nanotechnology **21**, 8 (2010).
[5] D. G. Yu, W. C. Lin, C. H. Lin, L. M. Chang, and M. C. Yang, Mater. Chem. Phys. **101**, 93 (2007).
[6] T. Qiu, X. L. Wu, J. C. Shen, P. C. T. Ha, and P. K. Chu, Nanotechnology **17**, 5769 (2006).
[7] P. Maksymovych, S. Jesse, P. Yu, R. Ramesh, A. P. Baddorf, and S. V. Kalinin, Science **324**, 1421 (2009).
[8] S. W. Han, M. H. Lee, and J. Ihm, Phys. Rev. B **65**, 085405 (2002).
[9] H. Jiang, J. Q. Hu, F. Gu, and C. Z. Li, Nanotechnology **20**, 055706 (2009).
[10] P. Deb, H. Kim, Y. X. Qin, R. Lahiji, M. Oliver, R. Reifenberger, and T. Sands, Nano Letters **6**, 2893 (2006).
[11] W. I. Park, G. C. Yi, J. W. Kim, and S. M. Park, Appl. Phys. Lett. **82**, 4358 (2003).
[12] J. Yu, M. Shafiei, W. Wlodarski, Y. X. Li, and K. Kalantar-Zadeh, J. Phys. D-Appl. Phys. **43**, 025103 (2010).
[13] T. A. Xia, Q. Li, X. D. Liu, J. A. Meng, and X. Q. Cao, J. Phys. Chem. B **110**, 2006 (2006).
[14] X. L. Li, J. F. Liu, and Y. D. Li, Appl. Phys. Lett. **81**, 4832 (2002).
[15] See supplementary material at http://dx.doi.org/10.1063/.... for tables and figures of the I. Deposition and characterization results; II. Comparison of field emission properties; and III. Barrier height calculations from both reverse and forward bias conditions.
[16] P. W. Voorhees, J. Stat. Phys. **38**, 231 (1985).
[17] C. J. Lee, T. J. Lee, S. C. Lyu, Y. Zhang, H. Ruh, and H. J. Lee, Appl. Phys. Lett. **81**, 3648 (2002).
[18] G. D. Wei, W. P. Qin, D. S. Zhang, G. F. Wang, R. J. Kim, K. Z. Zheng, and L. L. Wang, J. Alloys and Compounds **481**, 417 (2009).
[19] R. H. Fowler and L. Nordheim, Proceedings of the Royal Society of London Series a-Containing Papers of a Mathematical and Physical Character **119**, 173 (1928).
[20] T. Matsushima, Y. Kinoshita, and H. Murata, Appl. Phys. Lett. **91**, 253504 (2007).
[21] S. Sze and K. Ng, Physics of Semiconductor Devices, 3rd ed. (Wiley, 2008).
[22] J. Yu, S. J. Ippolito, M. Shafiei, D. Dhawan, W. Wlodarski, and K. Kalantar-zadeh, Appl. Phys. Lett. **94**, 013504 (2009).
[23] J. Appenzeller, M. Radosavljevic, J. Knoch, and P. Avouris, Phys. Rev. Lett. **92**, 048301 (2004).